

Stability of Two-Layered Earth Slope Under Varying Rainfall Intensity



Dooradarshi Chatterjee and A. Murali Krishna

Abstract Rainfall is one of the major causes of slope failures occurring in residual soils, which are of concern to geotechnical engineers. Naturally, soil is non-homogeneous in nature with different mechanical and hydraulic properties such as shear strength, soil–water characteristic curve, saturated permeability and unsaturated permeability functions. Negative pore-water pressure or matric suction plays an important role in the evaluation of stability of earth slopes. With rainfall infiltration, the pore-water pressure changes and hence affects its stability. A numerical model of a two-layered non-homogeneous slope is prepared with different hydraulic properties. An unsaturated seepage analysis with infiltration is performed in the finite element framework. With the pore pressures obtained from the seepage analysis, a finite slope stability analysis is performed in the limit equilibrium framework. The pore-water pressure profiles of the two-layered slope are studied with different rainfall intensities. The negative pore-water pressures are reduced to zero at a much shallow depth for higher rainfall intensity, thus reducing its safety factor rapidly. It is also observed that at high rainfall intensity, the two-layered slope suffers a shallow slope failure.

Keywords Non-homogeneous slope · SWCC · Pore-water pressure · Critical slip surface

1 Introduction

Slopes are non-homogeneous due to different mechanical properties and hydraulic properties like saturated permeability and unsaturated permeability function. Researchers have considered non-homogeneity in two ways, the first is lithological heterogeneity and the second is the spatial soil variability. Kim et al. [8] compared the stability of non-homogeneous slopes with different soil profiles using finite

D. Chatterjee (✉) · A. Murali Krishna
Indian Institute of Technology Guwahati, Guwahati, India
e-mail: dooradarshi@iitg.ac.in

© Springer Nature Singapore Pte Ltd. 2020
A. Prashant et al. (eds.), *Advances in Computer Methods and Geomechanics*, Lecture Notes in Civil Engineering 56,
https://doi.org/10.1007/978-981-15-0890-5_31

373

element limit analysis and limit equilibrium method. Qian et al. [12] proposed stability charts for two-layered cohesive slopes with depth factors ranging from 1.5 to 5. Chatterjee and Krishna [2] performed stability analysis of two-layered slopes with different soil combinations and showed how slip surfaces change with fine-grained and coarse-grained soils.

Slopes can be considered non-homogeneous with respect to the saturation levels occurring within the slope. In the event of rainfall, the saturation and moisture content vary highly within the slope. Failure of slopes is attributed to rainfall events more than any other causes. Gasmo et al. [7] developed numerical models to study infiltration within a slope and its effect on stability of the slope. Cho and Lee [3] studied the effect of infiltration using a two-dimensional finite element flow-deformation coupled analysis program. Zhang et al. [18] explained how under certain conditions matric suction in a slope is maintained even under rainfall infiltration. Rahardjo et al. [13] conducted a series of parametric studies under various rainfall intensities to study the influence of soil properties, initial groundwater table location and slope geometry on the stability of a residual soil slope. They concluded that the primary causes of instability of the slope were soil properties and rainfall intensity while water table location and slope geometry played a secondary role. Cho [4] used a one-dimensional infiltration model with an infinite slope to formulate an approximate method for evaluating the surficial stability of two-layered slopes. Yubonchit et al. [17] performed parametric studies within the finite element framework to observe the effects of slope angle, antecedent rainfall and saturated permeability on the stability of a shallow slope. The effect of rainfall intensity on the stability of a homogeneous slope is well established. However, the studies on non-homogeneous slopes are scarce. Therefore, a two-layered non-homogeneous slope is modelled with different rainfall intensities applied on the surface. The results obtained are analysed and illustrated through pore-water pressure profiles, safety factors and critical slip surfaces.

2 Problem Statement and Theory

A two-layered slope model as shown in Fig. 1 is considered for the study. A layer of top soil of 2 m thickness, representing relatively less permeable (Soil-2) material due to weathering is adopted. The slope angle is 35° and the slope height is 10 m. The front extent is taken as 30 m in front of the toe while the portion behind the crest is taken as 45 m. The initial groundwater table exists at a height of 10 m on the right side from the bottom and 5 m on the left side.

Slope stability analysis is performed followed by a transient seepage analysis in SLIDE v.8 [14]. The pore pressures from the seepage analysis are used as the initial condition for the stability analysis. The slope stability analysis was performed using

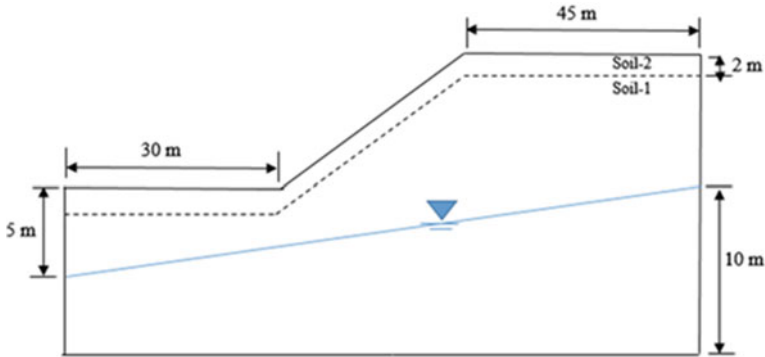


Fig. 1 Non-homogeneous two-layered slope model

the Morgenstern and Price [10] method with a half-sine function. A random search procedure [9] was used to obtain the minimum factor of safety of the slope.

The governing partial differential equation obtained from Darcy’s Law and the law of conservation of mass or continuity principle, for the flow of water through a two-dimensional unsaturated soil is represented by Eq. (1) [6]

$$\frac{\partial}{\partial x} \left(k_x \frac{\partial h}{\partial x} \right) + \frac{\partial}{\partial z} \left(k_z \frac{\partial h}{\partial z} \right) + q = \frac{\partial \theta}{\partial t} \tag{1}$$

where k_x and k_z are the hydraulic conductivities in the x- and z-directions, respectively, q is the applied flux and θ is the volumetric water content.

The soil–water characteristic curve (SWCC) or soil–water retention curve (SWRC) formulated by Van Genuchten [15] represents partially saturated soil behaviour in a very simple way as represented by Eq. (2).

$$\theta = \theta_r + \frac{\theta_s - \theta_r}{[1 + (\alpha h)^n]^m} \tag{2}$$

where θ is the volumetric water content; θ_s is the saturated water content; θ_r is the residual water content; h , the pressure head (matric suction) is positive; α is the inverse of the air entry value; n and $m = 1 - 1/n$ are curve fitting parameters. The hydraulic conductivity K is predicted using the statistical pore size distribution model of Mualem [11] illustrated by Eq. (3).

$$K = K_s S_e^{1/2} \left[1 - \left(1 - S_e^{1/m} \right)^m \right]^2 \tag{3}$$

$$S_e = \frac{\theta - \theta_r}{\theta_s - \theta_r} \tag{4}$$

The extended Mohr–Coulomb failure criterion uses effective cohesion, c' , net normal stress, $(\sigma - u_a)$, and matric suction, $(u_a - u_w)$ to represent shear strength in unsaturated soils. Fredlund et al. [5] proposed the extended model in the form of Eq. (5).

$$\tau = c' + \sigma' \tan \phi' + \psi \tan \phi^b \tag{5}$$

Where $\sigma' = \sigma - u_a$, $\psi = u_a - u_w$ and $\phi^b =$ parameter controlling increase in shear strength with suction.

3 Material Properties

To model the slope in this study, two different soils were selected. The soils were obtained from the field. From various laboratory tests, Soil-1 was classified as silty clay while Soil-2 as silty sand. Hydraulic conductivity of Soil-1 is less than Soil-2. The strength properties of the two soils are tabulated in Table 1.

Two experimental SWCC data were taken from Bordoloi et al. [1], corresponding to Soil-1, and Soil-2 in the present study. The Soil–water characteristic curves and unsaturated permeability functions of the two soils are represented by Van Genutchen function Van Genutchen [15] and Mualem [11]. The van Genutchen parameters (α, n, m, θ_s) were obtained (Table 2) using the optimization program RETC [16]. The Soil–water characteristic curves are shown in Fig. 2a and the permeability functions are shown in Fig. 2b.

Table 1 Mechanical Properties of soils used in study

Soil type	γ (kN/m ³)	c' (kPa)	ϕ' (°)	ϕ^b (°)
Soil-1	17.6	10	30	30
Soil-2	16.8	0	36	36

Table 2 Soil parameters used to evaluate SWCC and permeability functions

Soil type	a	n	m	θ_s	k_s (m/s)
Soil-1	0.005	1.26	0.21	0.43	8.38×10^{-6}
Soil-2	0.065	1.22	0.18	0.22	6.6×10^{-5}

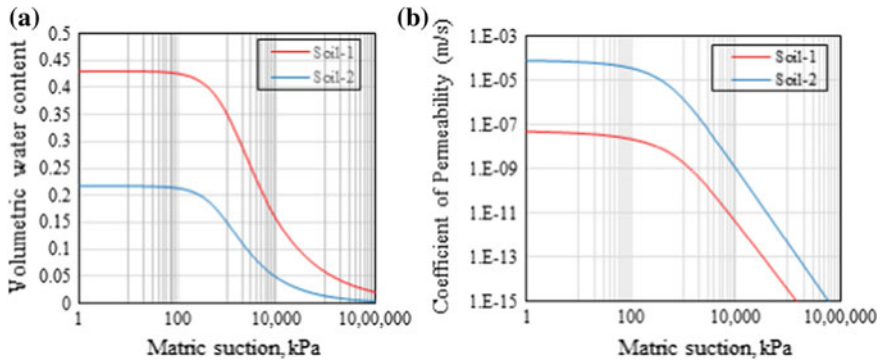


Fig. 2 a SWCC of the two soils used in the study and b permeability functions of the two soils used

4 Numerical Model

A numerical model of non-homogeneous slope (Fig. 3) has been prepared to study stability of slopes under rainfall infiltration. Finite element model was used in software SLIDE v8 [14] to perform the steady-state and transient seepage analysis. A constant head boundary condition was applied below the water table on both the sides of the slope. The portion of the boundary above the water table was specified as zero nodal flux boundary. To simulate rainfall, the slope surface was specified as flux equal to rainfall intensity. Five different rainfall intensities of 10, 30, 50, 100 and 200 mm/h were used. A short duration (24 h) rainfall was applied to the slope surface. To represent pore-water pressure profiles, section Y-Y at the middle of the slope is considered.

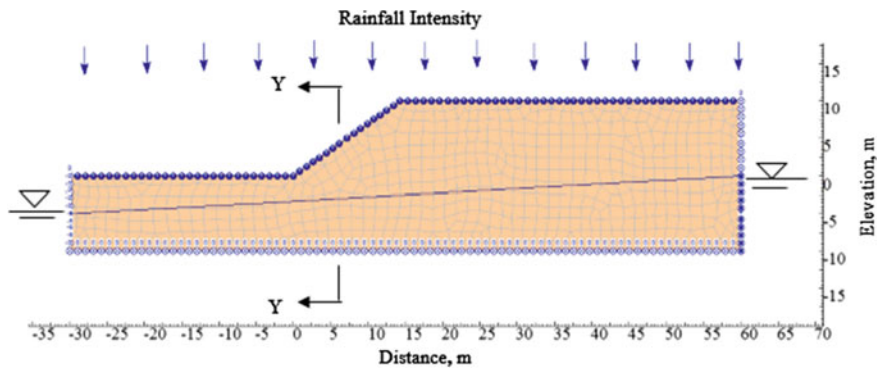


Fig. 3 Numerical model of slope

5 Results and Discussion

Figure 4 illustrates the pore pressure profiles of the two-layered slope at different rainfall intensities. The pressure profiles at the initial stage illustrate hydrostatic conditions within the slope mass. Figure 4a shows the pore pressure profile under 10 mm/h rainfall intensity. At the surface, the suction changes from 72 kPa at the initial stage to 42 kPa after 24 h and 59 kPa after 48 h. With rainfall infiltration, the profile shifts towards the right (positive pore pressures), i.e., suction decreases which results in a decrease in strength of the soil. As rainfall infiltration stops, the profile shifts left towards the initial position. Under 50 mm/h intensity (Fig. 4b), the 24th hour profile exhibit positive pore pressures throughout. There is no suction at all at this stage but with cessation of infiltration, the suction regains some of its value to 33 kPa after 48 h at the surface. Similarly, for 100 mm/h intensity (Fig. 4c), there is no suction after 24 h. The suction at the initial stage is 71 kPa at the surface, which becomes zero after 24 h but with stoppage of rainfall, it increases to 28 kPa. Figure 5 represents the pore pressure profiles of the mid-slope section after 24 h for different rainfall intensities. It is observed that the lowest rainfall intensity possess the maximum suction at the surface. As the intensity increases, the surface suction begins to reduce rapidly. The top 2 m of the pressure profiles indicates gradual reduction of suction but at more depth, the drop is almost vertical until the water level. Under 50 mm/h rainfall intensity, the pressure is positive throughout the depth. The pressure profiles for 100 and 200 mm/h follow the same path depicting that the soil has reached saturation.

Figure 5 depicts the pore-water pressure profiles of the two-layered slope under various rainfall intensities. As the rainfall intensity increases, the surface suction begins to reduce rapidly. Figure 6 represents the pore-water pressure contours within the two-layered slope. The negative pore pressure is maximum for rainfall intensity 10 mm/h whose factor of safety is also the maximum at 2.183. The water

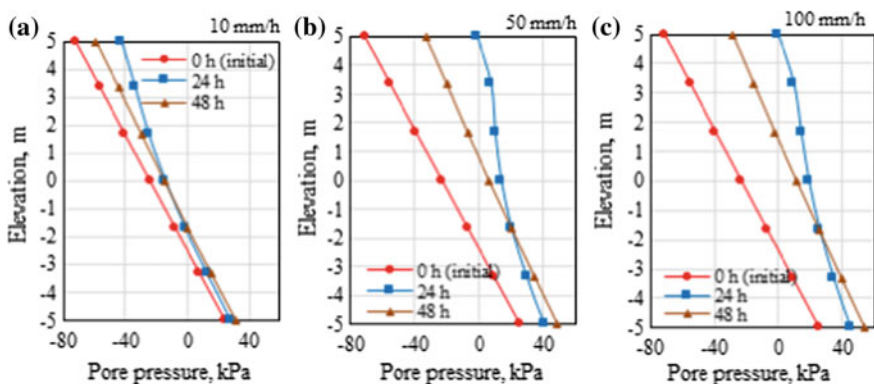
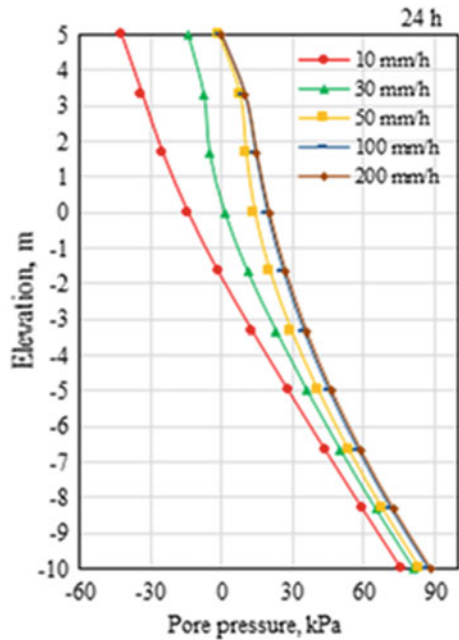


Fig. 4 Pore-water pressure profiles for the slope at different times under different intensities: **a** 10 mm/h, **b** 50 mm/h and **c** 100 mm/h

Fig. 5 Pore-water pressure profiles under different rainfall intensity after 24 h



just passes under the toe of the slope. The water level touches the slope surface under 30 mm/h rainfall intensity bringing the safety factor down to 1.364. A perched water table is formed under the 50 mm/h rainfall intensity. With an increase in rainfall intensity, the suction in the slope decreases and with it the safety factor as well.

The suction is in the range of 29–6 kPa for 50 mm/h rainfall intensity when the safety factor recorded is 0.721. At 100 mm/h, the maximum suction is in the range of 6–0 kPa with a safety factor of 0.59. The water now passes through the slope surface as run-off indicating that the soil has reached its infiltration capacity. After this stage, with more rainfall intensity, there is no effect on the pore pressures and the safety factor is similar at 0.587. WT represents the water table within the slope. The variation of factor of safety with rainfall intensity is illustrated in Fig. 7. The curve for 10 mm/h represents that the stability of the slope is not much affected because now the intensity is low as compared to the permeability of the soils. Hence, there is not much infiltration occurring to reduce the suction within the slope. With the increase in rainfall intensity, at 30 mm/h (nearly equal to permeability of Soil-1), the safety factor reduces to 1.364 after 24 h and reaching failure conditions (FS-0.928) after 48 h. The slope reaches failure conditions (FS-0.801) under 50 mm/h rainfall intensity just after 20 h of rainfall. The slope fails (FS-0.828) just after 5 h of rainfall while the safety factor is 0.679 after 5 h under 200 mm/h rainfall. The minimum factors of safety under the 100 mm/h and 200 mm/h rainfall intensity are similar which indicates the attainment of threshold

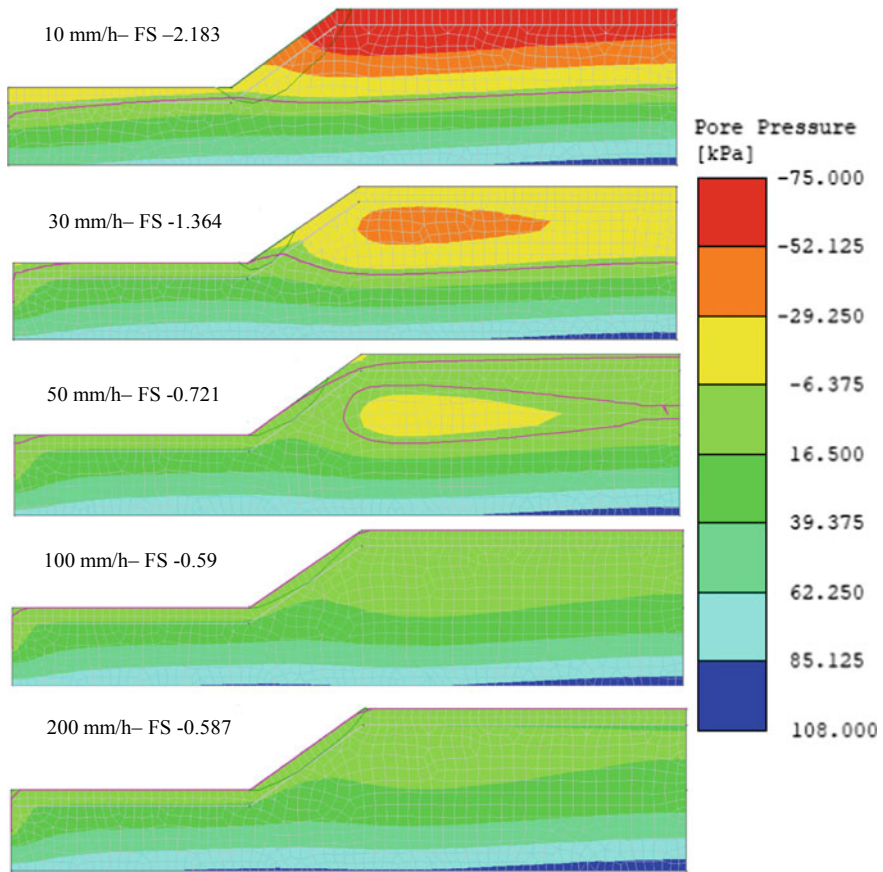


Fig. 6 Pore-water pressure contours under different rainfall intensity after 24 h

rainfall intensity. As rainfall stops, the slope recovers some safety factor with increase in suction.

Figure 8 depicts the critical slip surfaces for the slope at different rainfall intensities at initial stage, after 24 and 48 h. From Fig. 8a, it is observed that the slip surface at the initial stage and after 48 h follow same paths but the slip surface shifts towards the surface after 24 h due to water infiltrating during this time. The same phenomenon is observed under the 50 mm/h rainfall (Fig. 8b) when the slip surface after 24 h shifts towards the surface with a very shallow depth possessing a factor of safety of 0.721. With rainfall infiltration, the water reduces the effective cohesion within the soil and as a result, the critical surface becomes shallow with a reduced factor of safety. Under 100 mm/h intensity (Fig. 8c), the critical slip surface comes near the slope surface with a factor of safety of 0.59. At 200 mm/h rainfall intensity (Fig. 8d), similar slip surface is observed with a similar safety

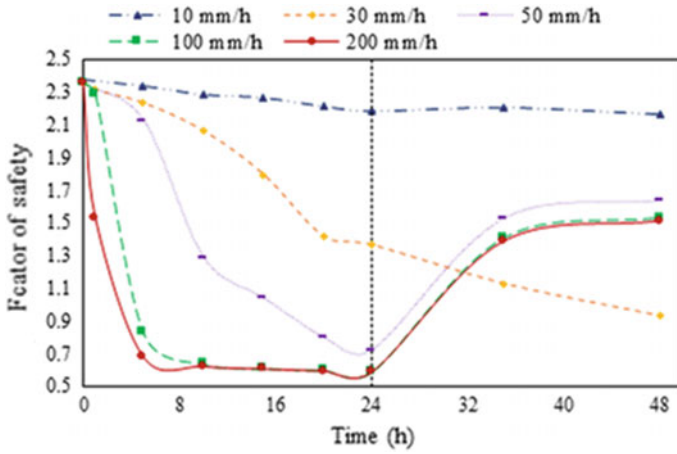


Fig. 7 Variation of safety factor with rainfall intensity

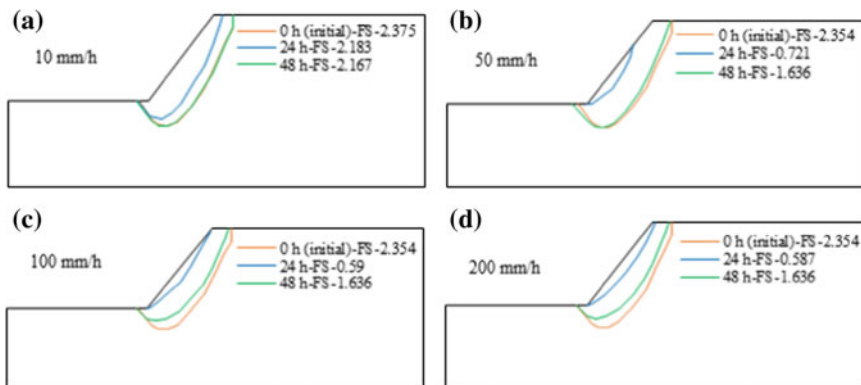


Fig. 8 Critical slip surfaces at different rainfall intensities 10, 50, 100 and 200 mm/h

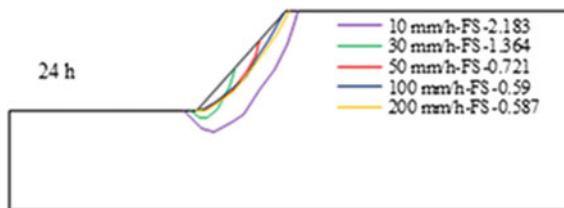


Fig. 9 Critical slip surfaces after 24 h for different rainfall intensities

factor denoting that the slope has reached its infiltration capacity where no effect will be observed with more increase in rainfall intensity.

Comparison of the critical slip surfaces under different rainfall intensities after 24 h is shown in Fig. 9. The slip surfaces for all the intensities represent shallow slope failure except the 10 mm/h intensity. The slip surfaces gradually extend towards the crest region with an increase in rainfall intensity from 30 to 200 mm/h.

6 Conclusions

Two-layered non-homogeneous slopes were modelled consisting of two soils of different saturated permeability and unsaturated permeability functions. From the results, it can be concluded that once the rainfall intensity exceeds the permeability of the soil, then only there is considerable change in suction, factor of safety and critical slip surface of the slope. With increase in rainfall intensity, the rate of decrease of suction increases and consequently the factor of safety. The critical slip surface starts moving towards the surface of the slope due to the decrease in effective cohesion of the soil. After the infiltration capacity of the soil is reached, run-off starts and there is no further change in the pore-water pressures within the slope.

References

1. Bordoloi S, Yamsani SK, Garg A, Sreedeeep S (2018) Critical Assessment of infiltration measurements for soils with varying fine content using a mini disk infiltrometer. *J ASTM Int* 47(2)
2. Chatterjee D, Krishna AM (2018) Stability analysis of two-layered non-homogeneous slopes. *Int J Geotech Eng* 5(1):1–7
3. Cho SE, Lee SR (2001) Instability of unsaturated soil slopes due to infiltration. *Comput Geotech* 28(3):185–208
4. Cho SE (2009) Infiltration analysis to evaluate the surficial stability of two-layered slopes considering rainfall characteristics. *Eng Geol* 105(3):32–43
5. Fredlund DG, Morgenstern NR, Widger RA (1978) The shear strength of unsaturated soils. *Can Geotech J* 15(3):313–321
6. Fredlund DG, Rahardjo H (1993) *Unsaturated soil mechanics*. Wiley, New York
7. Gasmu JM, Rahardjo H, Leong EC (2000) Infiltration effects on stability of a residual soil slope. *Comput Geotech* 26(2):145–165
8. Kim J, Salgado R, Lee J (2002) Stability analysis of complex soil slopes using limit analysis. *J Geotech Geoenviron Eng* 128(7):546–557
9. Malkawi AIH, Hassan WF, Sarma SK (2001) Global search method for locating general slip surface using Monte Carlo techniques. *J Geotech Geoenviron Eng* 127(8):688–698
10. Morgenstern NR, Price VE (1965) The analysis of the stability of general slip surfaces. *Geotechnique* 15(1):79–93
11. Mualem Y (1976) Hysteretical models for prediction of the hydraulic conductivity of unsaturated porous media. *Water Resour Res* 12(6):1248–1254

12. Qian ZG, Li AJ, Merifield RS, Lyamin AV (2014) Slope stability charts for two-layered purely cohesive soils based on finite-element limit analysis methods. *Int J Geomech* 15(3):1–14
13. Rahardjo H, Ong TH, Rezaur RB, Leong EC (2007) Factors controlling instability of homogeneous soil slopes under rainfall. *J Geotech Geoenviron Eng* 133(12):1532–1543
14. Rocscience (2018) SLIDE (v8). Toronto, Canada: Rocscience Inc
15. Van Genuchten MT (1980) A closed-form equation for predicting the hydraulic conductivity of unsaturated soils. *Soil Sci Soc Am J* 44:892–898
16. Van Genuchten MT, Leij FJ, Yates SR (1991) The RETC code for quantifying the hydraulic functions of unsaturated soils. U.S. Environmental Protection Agency, Ada, Oklahoma
17. Yubonchit S, Chinkulkijniwat A, Horpibulsuk S, Jothityangkoon C, Arulrajah A, Suddeepong A (2017) Influence factors involving rainfall-induced shallow slope failure-numerical study. *Int J Geomech* 17(7):1–13
18. Zhang LL, Fredlund DG, Zhang LM, Tang WH (2004) Numerical study of soil conditions under which matric suction can be maintained. *Can Geotech J* 41(4):569–582